Cell Reports
Physical Science

CellPress
OPEN ACCESS

Article

Modified layered double hydroxides for efficient and reversible carbon dioxide capture from air

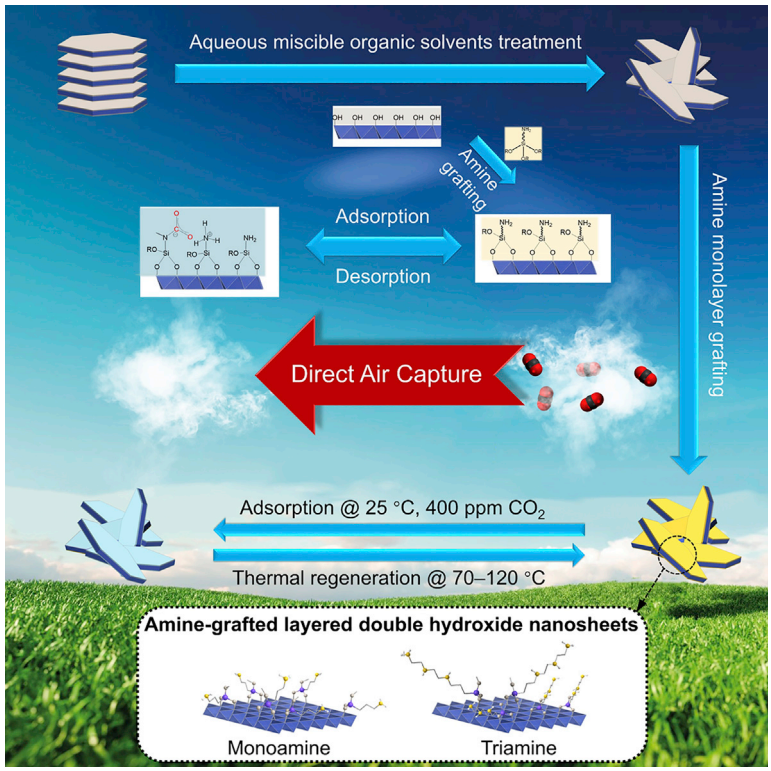

Zhu et al. synthesize modified layered double hydroxides (LDHs) to capture CO_2 from ambient air. Exposed hydroxyl groups on LDHs react with aminosilanes to form amine monolayer grafted nanosheets, allowing ultrafast CO_2 capture. Platelet size, thickness, and exfoliated morphology have a significant impact on obtaining the optimal amine grafting.

Xuancan Zhu, Meng Lyu, Tianshu Ge, ..., Fan Yang, Dermot O'Hare, Ruzhu Wang

baby_wo@sjtu.edu.cn (T.G.)
rzwang@sjtu.edu.cn (R.W.)

Highlights

Amine monolayer-tethered, exfoliated layered double hydroxides are synthesized

The adsorbent shows an CO_2 capacity of 1.05 mmol g^{-1} in simulated air

CO_2 uptake reaches 70% of this maximum capacity within 30 min

Negligible performance degradation is observed after 50 cycles

Zhu et al., Cell Reports Physical Science 2, 100484
July 21, 2021
https://doi.org/10.1016/j.xcrp.2021.100484

Cell Reports
Physical Science

CellPress
OPEN ACCESS

Article

Modified layered double hydroxides for efficient and reversible carbon dioxide capture from air

Xuancan Zhu,[1] Meng Lyu,[2] Tianshu Ge,[1,*] Junye Wu,[1] Chunping Chen,[2] Fan Yang,[1] Dermot O'Hare,[2] and Ruzhu Wang[1,3,*]

SUMMARY

Direct air capture (DAC) is becoming a technically feasible negative emission technology; however, the fabrication of affordable adsorbents with large CO_2 capacities, fast kinetics, and high sorption-desorption stability are of critical importance for the large-scale deployment of the DAC process. In this study, amine functionalized, aqueous miscible organic Mg_xAl-CO_3 layered double hydroxide (LDH) nanosheets are used to efficiently and rapidly capture CO_2 from ambient air. 3-[2-(2-Aminoethylamino)ethylamino]propyl-trimethoxysilane (TRI) treatment of highly dispersed LDH nanosheets produces a sorbent exhibiting an impressive adsorption capacity of 1.05 mmol g^{-1} at 25°C when exposed to 400 ppm CO_2, which is 30% higher than equivalent amine-functionalized SBA-15 supports. CO_2 uptake reaches 70% of this maximum capacity within 30 min and is twice as fast as supported polyamines. The highly dispersed LDH nanosheets provide excellent thermal, hydrothermal, and chemical stability, with negligible performance degradation after 50 adsorption-desorption cycles.

INTRODUCTION

Fossil fuels are still the world's primary energy source, with global carbon dioxide (CO_2) emissions totaling ~35 Gt annually.[1] Integrated assessment models suggest that to ensure that the global mean temperature increase stays within 2°C by the end of the 21st century, CO_2 capture rates should reach 5–23 Gt $year^{-1}$ by 2050, and 8–50 Gt $year^{-1}$ by 2100.[2] To aim for the more stringent target of 1.5°C, even negative emission technologies with cumulative CO_2 capacities of 400–800 Gt are required.[3] Direct air capture (DAC) by absorption/desorption with subsequent storage or utilization provides efficient negative emissions to remove atmospheric CO_2 to attenuate the use of fossil fuels and build a closed carbon cycle. Absorption-based DAC pilot plants using alkali metal hydroxide solvents operate at low costs (94–232 USD [US dollars] t_{CO2}^{-1}) but face significant water loss and high regeneration temperatures. In contrast, a recent study indicated that the large-scale deployment of DAC by adsorption is now technically and economically feasible to achieve the ambitious goal of capturing 1% of annual global CO_2 emissions.[4] Nevertheless, DAC is in its early stages, and the development of affordable adsorbents with large loading capacities, fast kinetics, and minimal degradation rates is of critical importance to reduce the capital required and the operating and maintenance costs of DAC processes.[5]

Amine-functionalized porous materials are the most attractive adsorbents for CO_2 capture from dilute and ultradilute conditions.[6–8] Under dry conditions, two amine

[1]Research Center of Solar Power & Refrigeration, School of Mechanical Engineering, Shanghai Jiao Tong University, 800 Dongchuan Road, Shanghai 200240, China

[2]Chemistry Research Laboratory, Department of Chemistry, University of Oxford, 12 Mansfield Road, Oxford OX1 3TA, UK

[3]Lead contact

*Correspondence: baby_wo@sjtu.edu.cn (T.G.), rzwang@sjtu.edu.cn (R.W.)

https://doi.org/10.1016/j.xcrp.2021.100484

groups can react with one CO_2 molecule to reversibly form ammonium carbamates. Unfortunately, effective amine efficiencies (mol of CO_2 captured/mol of N atoms) of DAC adsorbents are considerably lower than the theoretical maximum of 0.5, especially for class 1 adsorbents prepared by the physical impregnation of polyamines. The low amine efficiency is mainly ascribed to the disordered stacking of amines, which blocks the active sites and slows the rate of CO_2 diffusion. In addition, the long-term stability of class 1 adsorbents with respect to thermal regeneration and in the presence of oxygen is also of concern because of the weak interaction between the amines and supports.[9] Therefore, extensive efforts have been devoted to developing class 2 adsorbents that strongly tether small amine molecules onto supports through covalently chemical bonds.[10]

Class 2 adsorbents can be prepared either by the silylation of hydroxyl groups, or, in rare cases, by cross-coupling reactions. In general, primary amines yield higher amine efficiency than secondary and tertiary amines under gas flows of 400 ppm CO_2 because of an entropic effect,[11,12] which leads to the extensive use of amine compounds such as 3-aminopropyltrimethoxysilane (APS). By varying the length of the organic linker from one to five carbon atoms in the primary amine, the propyl linker of APS was found to provide sufficient flexibility to capture CO_2 molecules between two neighboring amines.[13] However, the low nitrogen content of supported monoamines limits the overall CO_2 capacities, and therefore, multiple amines on a linker may be more attractive for amine grafting. Notably, the amine loadings of supported 3-[2-(2-aminoethylamino)ethylamino]propyl-trimethoxysilane (TRI) monolayers and multilayers reach up to 6.2 and 7.9 mmol g^{-1}, respectively.[14,15] Further studies demonstrated the cyclic stability of TRI-grafted adsorbents for DAC in temperature swing operation with steam purge to concentrate desorbed CO_2.[16,17] It should be noted that although branched aminosilanes such as bis(2-aminoethyl)amine (B-ethyl) and bis(2-aminopropyl)amine (B-propyl) containing mainly primary amines lead to higher amine efficiency, linear aminosilanes containing both primary and secondary amines can be more densely grafted onto the supports due to less steric hindrance.[18] The long alkyl chains in linear aminosilanes provide a propensity to achieve intramolecular CO_2 adsorption.

The efficient assembly of class 2 adsorbents also relies on obtaining appropriate supports with high surface areas, tunable pore structures, and abundant hydroxyl groups on the surface. Most class 2 adsorbents for CO_2 adsorption use ordered mesoporous silica supports such as Mobil composition of matter no. 41 (MCM-41),[14] pore-expanded MCM-41 (PE-MCM-41),[16,17] MCM-48,[19] SBA-15,[13,20] and mesocellular foam (MCF).[11] The mass production of these supports is still inefficient and costly, and alternative amine grafting supports are highly sought after. Recently, a new family of DAC adsorbents was prepared by impregnating branched poly(ethyleneimine) (PEI) onto Mg_xAl-CO_3 layered double hydroxide (LDH)-derived mixed metal oxides (MMOs), achieving CO_2 capacities of up to 2.27 mmol g^{-1} in 400 ppm CO_2 in N_2 mixtures at 25°C.[21] The LDHs that were treated with aqueous miscible organic solvents (AMOST) during the co-precipitation process were successfully exfoliated into 2-dimensional (2D) nanosheets,[22–24] and subsequently self-assembled into spherical nanoparticles during vacuum calcination. Their unique flower-like morphology with abundant slit-shaped mesopores offers a loose framework for loading high amounts of PEIs (e.g., 67 wt%) with a low-performance degradation, while conserving the large surface area of LDH-derived nanosheets ensures that active sites remain accessible to CO_2. More important, LDH can be readily produced on a large scale and are accessible from cost-effective, commercially available earth-abundant chemicals. Typically, MgAl-LDHs are 2–3 USD kg^{-1}, and AMOST-

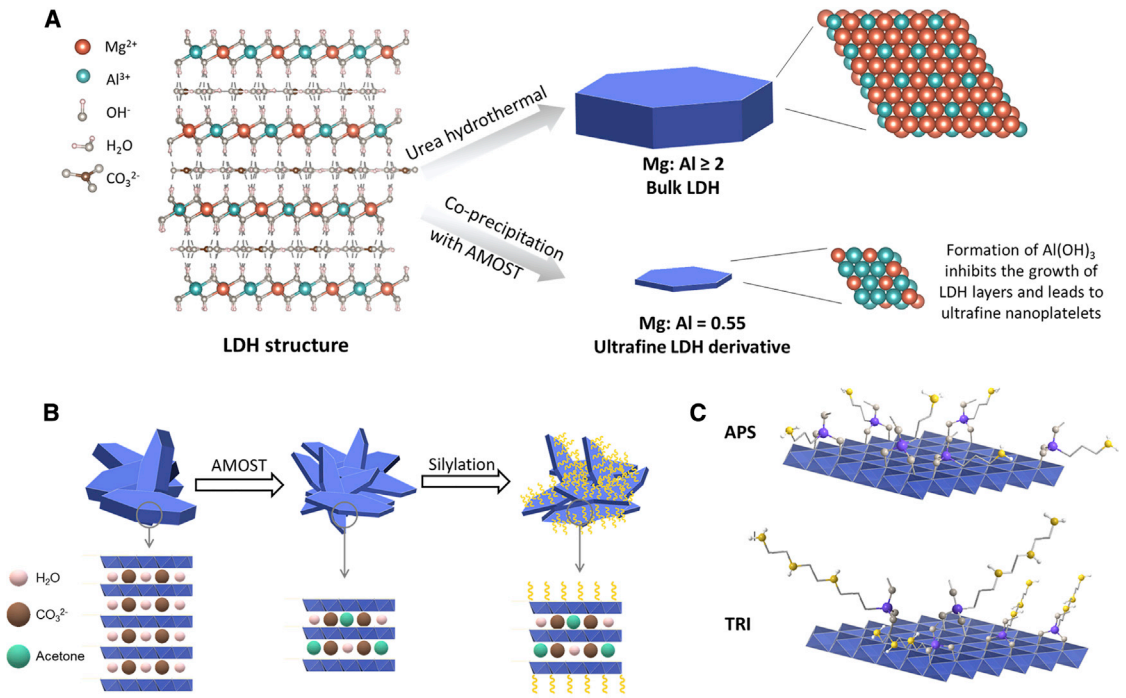

Scheme 1. The fabrication of amine monolayer grafted MgAl-LDHs

(A) Synthesis of bulk and ultrafine LDH-derived supports.

(B) Silylation process of AMOST-treated LDHs.

(C) Structure of monolayer-grafted amines.

treated LDHs (AMO-LDHs) add an additional cost of 5 USD kg^{-1}. The pelleting of LDH powders through either dry granulating or wet extrusion is also well established.[25,26] Considering that each metal cation in LDH-derived nanosheets is 6-fold coordinated by edge-sharing hydroxyl groups,[27] exfoliated LDHs may offer possibilities for high grafting densities of aminosilanes. Preliminary studies reported several examples of LDH silylation, while the amine loadings on LDHs have not been comprehensively investigated.[28,29]

Our preliminary modeling work indicates the great potential of improving the kinetics of adsorbents on decreasing the energy consumption of DAC processes and increasing CO_2 productivity.[30] Another research project from Lackner's group shows the importance of cyclic stability.[31] In this work, aminosilane monolayers were grafted onto the surface of exfoliated AMO-LDH-derived nanosheets and applied in DAC for the first time (Scheme 1). Amine monolayer-grafted LDHs are expected to exhibit superior kinetics and stability compared to PEI-impregnated MMOs because of the minimal change in the support morphology after amine modification. Platelet size and exfoliated LDH-derived nanosheets thickness determine the number of exposed hydroxyl groups on the surface accessible for grafting, and thus their effects on amine loading are reported. The advantages of using amine monolayer-grafted LDHs over current amine-functionalized adsorbents in CO_2 capture from air under moisture-free conditions are discussed in terms of capacities, kinetics, and stabilities.

RESULTS

Synthesis and characterization of supports and adsorbents

A series of Mg_xAl-CO_3 LDH-derived nanosheets with tailored sizes and thicknesses were prepared, and the Mg:Al molar ratio (x) was varied from 0.55 to 3. Transmission

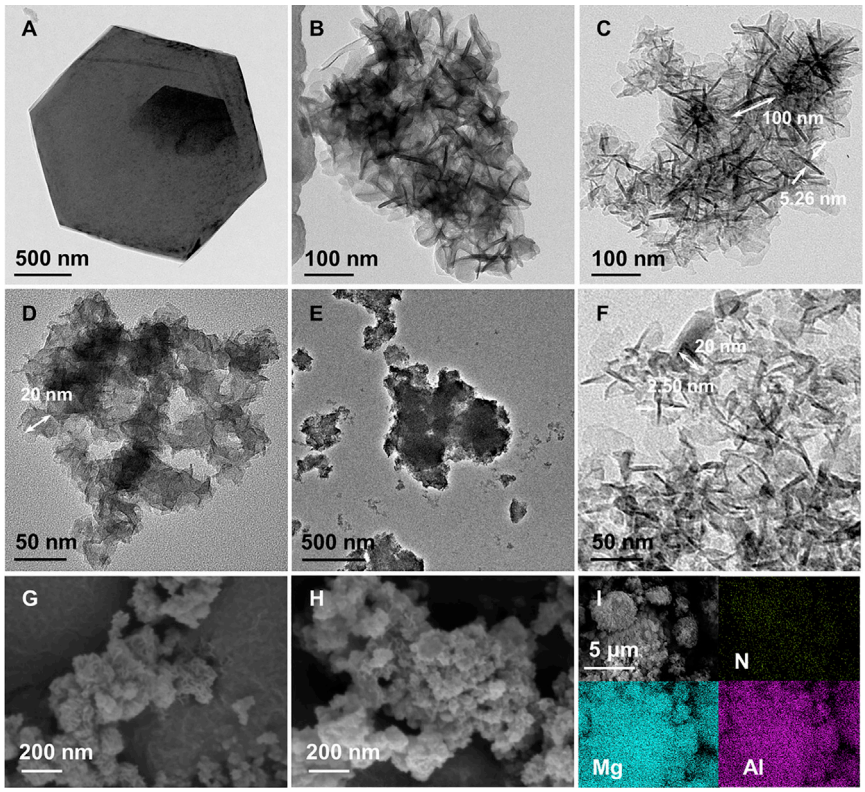

Figure 1. Morphologies of supports and adsorbents

(A) TEM image of Mg_2Al-urea.
(B) TEM image of Mg_2Al-w.
(C) TEM image of Mg_2Al-a.
(D) TEM image of Mg_2Al-a-F.
(E) TEM image of $Mg_{0.55}Al$-w.
(F) TEM image of $Mg_{0.55}Al$-a.
(G) SEM image of Mg_2Al-a-F.
(H) SEM image of TRI-Mg_2Al-a-F.
(I) Energy-dispersive spectroscopy scan of TRI-Mg_2Al-a-F with N:Mg:Al atomic ratio of 1.86:14.82:7.38.

electron microscopy (TEM) images (Figures 1A–1F) show that LDHs (denoted as Mg_xAl-urea) with a hexagonal platelet shape and particle size of 2 μm can be formed when the hydrothermal urea method was used. When the co-precipitation method was used at pH 10, a decrease in LDH lateral size to nanoscale was observed (denoted as Mg_xAl-w). Unfortunately, strong interlayer hydrogen bond networks result in a high degree of stacking in LDH-derived nanosheets, especially in the case of low Mg:Al ratios. AMOST treatment results in the replacement of the water between the layers with an AMO organic solvent and thus efficiently, although not completely, exfoliate LDHs into nanosheets after vacuum drying. For instance, the acetone-dispersed Mg_xAl-CO_3 LDHs (denoted as Mg_xAl-a) have lateral sizes of 20–100 nm, and the platelet thickness of Mg_2Al-a and $Mg_{0.55}Al$-a are ~5.26 and 2.50 nm, respectively. Note that the ultrafine and ultrathin dimensions of $Mg_{0.55}Al$-a nanosheets arise in part due to the formation of some $Al(OH)_3$ because of the low Mg:Al ratio.[21] Furthermore, fast coprecipitation followed by acetone washing (denoted as Mg_xAl-a-F) led to a further reduction in LDH lateral size.[24] However, these LDH-derived nanosheets are prone to fragmentation and stacking, possibly because of inadequate crystallization under variable pH conditions. Scanning electron microscopy

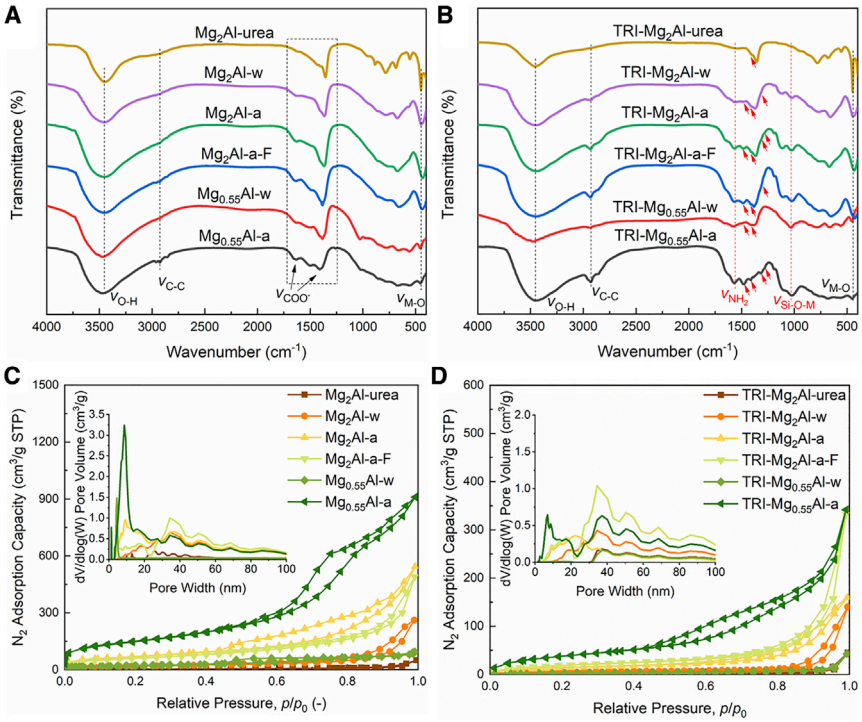

Figure 2. Material characterization of supports and adsorbens

(A) FTIR results for LDHs.

(B) FTIR results for TRI-grafted LDHs.

(C) N_2 adsorption-desorption isotherms at 77 K and density functional theory-based pore size distributions for LDHs.

(D) N_2 adsorption-desorption isotherms at 77 K and density functional theory-based pore size distributions for TRI-grafted LDHs.

(SEM) images also confirmed the formation of flower-like morphologies and abundant slit-shaped mesopores (Figures 1G and S1). These exfoliated LDH-derived nanosheets are expected to exhibit a substantial number of exposed hydroxyl groups suitable for amine grafting.

TRI was reacted with LDH nanosheets in toluene at 85°C for 16 h. The TRI-functionalized LDH nanosheets were separated by centrifugation, followed by washing with toluene, hexane, and methanol, and then dried under vacuum at 60°C. Multilayer grafting can be achieved only in the presence of water to consume the free alkoxy ligands and complete the surface coverage.[32,33] The TRI-functionalized LDHs (denoted by TRI-*y*, *y* = support) retained a flow-like morphology (Figure 1H); energy-dispersive spectroscopy (EDS) revealed a uniform distribution of N atoms throughout the samples (Figure 1I). Fourier-transform infrared spectroscopy (FTIR) showed that the supports prepared exhibited characteristic LDH bands (Figure 2A), including the O-H stretching vibration (3,450 cm^{-1}) of interlayer trapped water and surface-bound hydroxyl groups, alkyl group C-C stretching (2,925 cm^{-1}) and bending (1,490 cm^{-1}) vibrations, carboxylate symmetrical and asymmetrical stretching vibrations (1,635, 1,355–1,410 cm^{-1}), and M-O lattice vibrations (445 cm^{-1}).[34] The successful grafting of TRI molecules was confirmed by an increase in the C-C stretching and bending vibrations, as well as the appearance of NH_2 bending (1,560 cm^{-1}) and Si-O-M stretching (1,022 cm^{-1}) vibrations (Figure 2B). In addition, small absorbances in the 1,260–1,500 cm^{-1} region can be

ascribed to the alkylammonium carbamate ion pairs formed from CO_2 adsorption upon exposure to air.[35]

N_2 adsorption/desorption measurements at 77 K provided information about the surface area and pore structure of the samples. The LDH supports exhibit type IV isotherms with H3 hysteresis loops (Figures 2C and S2), which indicate slit-shaped mesopores structured by the LDH-derived nanosheets. In contrast to ordered mesoporous silica supports such as SBA-15 (Figure S2A), LDHs have a considerably broader pore size distribution (up to 100 nm), and pore volumes are inversely related to the size and thickness of the LDH-derived nanosheets. After grafting, the TRI molecules covered the surface of the mesopores with a depth ranging from 5 to 15 nm (Figures 2D and S3). The retention of large pore structures further suggests the monolayer dispersion of TRI on the surface of LDHs. The detailed textural properties of the samples are summarized in Table S1. Notably, TRI-$Mg_{0.55}$Al-a exhibited an impressive surface area of 162 $m^2\ g^{-1}$ and a pore volume of 0.553 $cm^3\ g^{-1}$, exceeding those of TRI-SBA-15 (96 $m^2\ g^{-1}$ and 0.231 $cm^3\ g^{-1}$, respectively) and remarkably higher than those of PEI-impregnated SBA-15 (PEI-SBA-15) and calcined $Mg_{0.55}$Al-a (PEI-$Mg_{0.55}$Al-a(c)).[21] The ideal morphologies of TRI-LDHs, with abundant slit-shaped mesopores as well as large surface areas and pore volumes, provide optimal access to amine actives sites for CO_2 adsorption.

CO_2 adsorption capacity of modified LDHs

We have measured the CO_2 adsorption isotherms at 25°C for all of the adsorbents prepared (Figure 3A). While the TRI-grafted bulk and stacked LDHs exhibited poor CO_2 capacities under ultradilute conditions, obvious improvements were observed for TRI-grafted AMO-LDHs. Remarkably, TRI-$Mg_{0.55}$Al-a achieved a CO_2 uptake capacity of 1.049 mmol g^{-1} upon exposure to 0.4 mbar CO_2, which is 16.7 times higher than that of TRI-$Mg_{0.55}$Al-w (0.063 mmol g^{-1}) and 30% higher than TRI-SBA-15 (0.808 mmol g^{-1}). The fast coprecipitation process did not significantly improve the capacity of TRI-LDHs, which indicates that both reduction in LDH size and thickness and morphology exfoliation play an important role in establishing the desired amine-grafting sites. The monoamine-grafted AMO-LDHs were also tested. They exhibit a very promising capacity of 0.416 mmol g^{-1} for APS-Mg_2Al-a and 0.778 mmol g^{-1} for APS-$Mg_{0.55}$Al-a in 0.4 mbar.

Considering the low physisorption capacities of the LDHs under 0.4 mbar at 25°C (Figure S4) and the decreased surface areas after amine grafting, the enhanced CO_2 capacity seen for TRI-LDHs is mainly attributed to chemisorption by the amine functional groups. The isosteric heat of adsorption of TRI-$Mg_{0.55}$Al-a samples was calculated according to the Clausius-Clapeyron relation from isotherms measured at 25°C, 45°C, and 65°C (Figures 3B and 3C). The heat of adsorption was underestimated at low CO_2 coverages, but quickly approached 79 kJ mol^{-1} and remained above 65 kJ mol^{-1} for loadings of up to 1.2 mmol g^{-1}, which is typical for CO_2 chemisorption on amines.[36] At higher surface coverages, physisorption dominates the adsorption process, with the heat of adsorption ranging from 15 to 40 kJ mol^{-1}.[35]

Elemental analysis was conducted to quantitatively measure the amine loading of the samples (Table S2). The near-zero elemental-N content in the LDH supports indicates that nitrates were effectively removed during washing. This guarantees the accuracy of using the N content in elemental analysis to evaluate amine loadings. The influence of the morphology of the LDH supports on TRI loadings is clearly observed; Mg_2Al-urea producing stone-like LDH platelet agglomerates can scarcely react with amine-based surface modifiers, whereas exfoliated AMO-LDHs exhibited

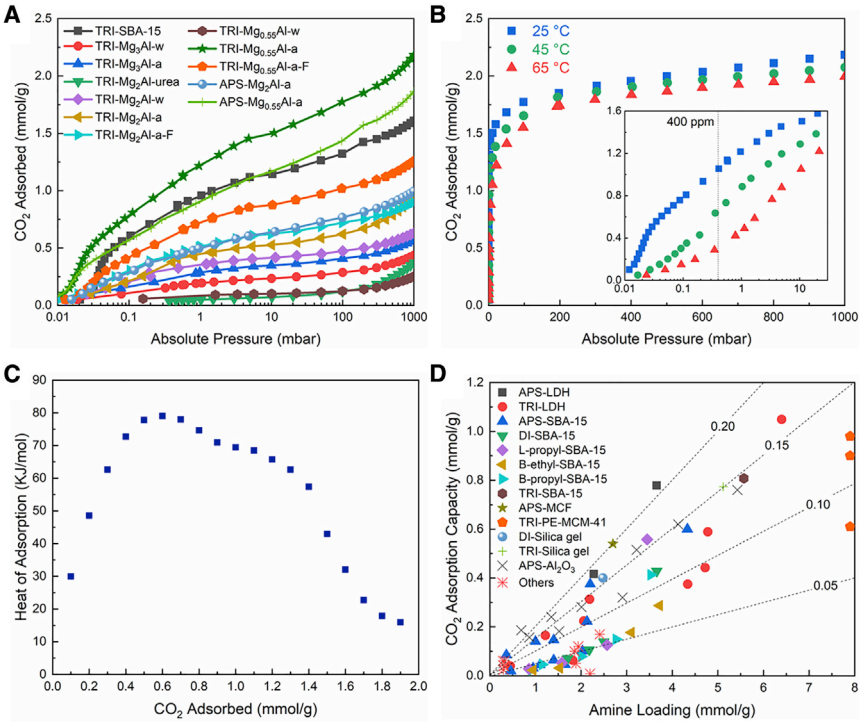

Figure 3. CO_2 adsorption capacity of modified LDHs

(A) Screening of CO_2 adsorption isotherms of amine-grafted samples at 25°C.

(B) CO_2 adsorption isotherms of TRI-$Mg_{0.55}$Al-a at 25°C, 45°C, and 65°C.

(C) Isosteric heats of adsorption onto TRI-$Mg_{0.55}$Al-a.

(D) CO_2 adsorption capacities under 0.4 mbar and 25°C as a function of amine loadings.

very high amine loadings of up to 6.399 mmol g^{-1}. The very low amine loading of TRI-grafted bulk LDH suggests it is highly unlikely that there is any multilayer grafting. The performance of all of the amine-grafted adsorbents for DAC under dry conditions is summarized in Table S3 and Note S1, and the molecular structures of the relevant aminosilanes are listed in Table S4. When correlating CO_2 adsorption capacity under 0.4 mbar with amine loading, it was found that the amine efficiency of TRI-LDHs fell in the range of 0.09 to 0.17 (Figure 3D). Promising amine loadings (6.399 mmol g^{-1}) and amine efficiency (0.164) were exhibited by TRI-$Mg_{0.55}$Al-a, improving on most class 2 adsorbents currently reported. The increase in amine efficiency of TRI-$Mg_{0.55}$Al-a compared to other TRI-LDHs with lower amine loadings can be attributed to an improved accessibility of the densely grafted amine active sites, with two neighboring amines binding one CO_2 molecule. The amine efficiency of TRI-LDHs appears not to be the limiting factor, with the increase of monolayer amine loading up to 6.399 mmol g^{-1}, and thus the optimal amine group distance cannot be determined. Higher amine loadings of 7.9 mmol g^{-1} were reported by Belmabkhout et al.[16] in TRI-PE-MCM-41; however, sample preparation by a water-assisted process in that work resulted in stacking of the amine multilayer. The resulting cross-linked array can easily block the support's mesopores, impairing CO_2 diffusion and lowering amine efficiency as well. Compared to TRI-grafted samples, APS-Mg_2Al-a and APS-$Mg_{0.55}$Al-a containing only primary amines achieved even higher amine efficiencies of 0.183 and 0.212, respectively. Reports of amine efficiencies exceeding 0.2 are rare in the literature—in most cases appearing when amine loadings are low and where physisorption of the remaining surface may significantly contribute to the overall capacity.[6]

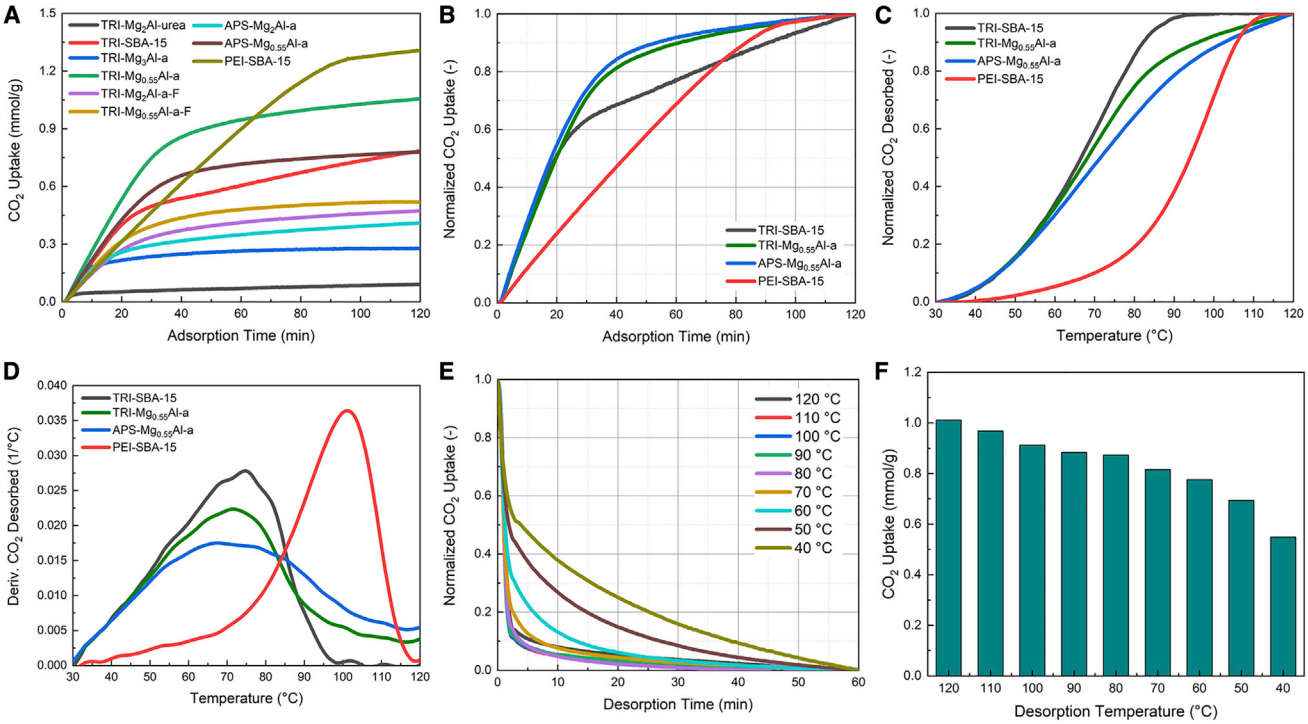

Figure 4. CO_2 adsorption and desorption kinetics of modified LDHs

(A) CO_2 uptakes of amine-grafted samples at 25°C under 400 ppm CO_2 in N_2 after regeneration at 120°C under pure N_2 for 60 min.

(B) Normalized CO_2 uptakes after division by the total CO_2 uptakes after 120 min.

(C) Normalized CO_2 desorbed from 25°C to 120°C at a heating rate of 5°C min^{-1} after saturation under 400 ppm CO_2.

(D) Temperature-programmed desorption (TPD) results calculated from the differential of normalized weight loss in C.

(E) Normalized CO_2 uptakes of TRI-$Mg_{0.55}$Al-a when regenerated at varying temperatures under pure N_2 for 60 min.

(F) CO_2 uptakes of TRI-$Mg_{0.55}$Al-a within 120 min at 25°C under 400 ppm CO_2 in N_2 after regeneration at varying temperatures under pure N_2 for 60 min.

Kinetics of modified LDHs

DAC adsorbents suffer from poor kinetics under ultradilute conditions, commonly requiring several hours for polyamine-impregnated adsorbents to reach half-adsorption capacities.[37] In contrast, Figure 4A shows that amine-grafted LDHs exhibited fast CO_2 adsorption rates when exposed to N_2 flow containing 400 ppm CO_2, and the CO_2 uptake within 120 min correlates with the capacities determined from isotherm tests. It is worth noting that TRI-$Mg_{0.55}$Al-a displayed an even higher CO_2 uptake within 60 min than the representative class 1 adsorbent PEI-SBA-15. Normalizing CO_2 uptake by dividing with the total CO_2 capacity (Figure 4B) gives more reliable comparisons, showing that both APS- and TRI-$Mg_{0.55}$Al-a reached 70% capacity within 30 min, whereas the time required was doubled for PEI-SBA-15 to reach the same capacity. The long diffusion process detected for TRI-SBA-15 further indicates the benefit of using LDH supports with a broader range of pore sizes to avoid amine blockages.

Amine-grafted LDHs also showed a decrease in desorption temperature peaks (e.g., 75°C) compared to PEI-SBA-15 (100°C), as evidenced by the temperature-programmed desorption (TPD) results at a heating rate of 5°C min^{-1} (Figures 4C and 4D). The milder regeneration requirements of amine-grafted LDHs provide the opportunity to use industrial waste heat at temperatures <100°C. For instance, TRI-$Mg_{0.55}$Al-a retained 80% of its total adsorption capacity, with a desorption temperature as low as 80°C (Figure 4C). It should be noted that amine monolayers formed

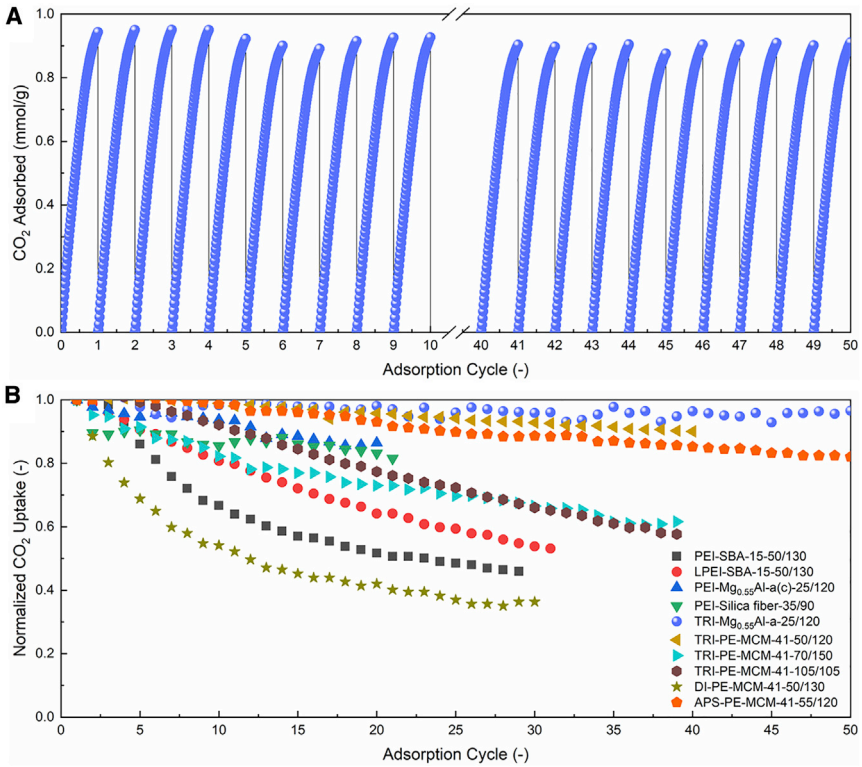

Figure 5. Stability of modified LDHs

(A) A 50-cycle test of TRI-$Mg_{0.55}$Al-a when adsorbed at 25°C in 400 ppm CO_2/N_2 for 60 min and desorbed at 120°C in pure N_2 for 15 min.

(B) Comparison of long-term stability of class 2 adsorbents under dry conditions.

by dry grafting dispersion on exfoliated LDH-derived nanosheets exhibited the lowest CO_2 desorption to gas stream pathway. In contrast, polyamine molecules thickened and aggregated on the support surface, and thus required additional energy to transfer desorbed CO_2 through amine films.[38] In addition, ultrafast CO_2 desorption kinetics were observed for TRI-$Mg_{0.55}$Al-a, which only required 70°C to regenerate 90% of the normalized CO_2 uptake in 10 min (Figures 4E and S5). After desorption under a range of temperatures, fast adsorption kinetics were retained in the next cycle (Figure S6), and CO_2 uptake within 120 min agreed well with the TPD results (Figure 4F).

Stability of modified LDHs

Taking advantage of their thermal, hydrothermal, and chemical stability, commercial opportunities for amine-modified LDHs with their promising adsorption capacities and kinetics could be an attractive option for rapid temperature swing adsorption (R-TSA) processes to significantly increase CO_2 productivity and reduce energy consumption in DAC.[30] To demonstrate this further, a 50-cycle test was carried out for TRI-$Mg_{0.55}$Al-a with adsorption at 25°C in 400 ppm CO_2/N_2 for 60 min followed by desorption at 120°C in pure N_2 for 15 min. Under these working conditions, TRI-$Mg_{0.55}$Al-a achieved an average CO_2 uptake of 0.912 mmol g^{-1} with high stability throughout all of the cycles (Figure 5A). The stability results were compared to the existing data in the literature marked as A-*X*/*Y*, where A, X, and Y represent the adsorbent, adsorption, and desorption temperatures, respectively (Figure 5B; Table S5). In general, amine-grafted adsorbents showed better cycling stability under dry conditions than polyamine-impregnated adsorbents because of lower amine leakage during heating. For instance, PEI-SBA-15-

50/130 loses >50% of the uptake after only 30 cycles.[39] Additional treatments, such as adding nanostructured compounds[40,41] or surface modification,[42–44] are required to strengthen the bond between the polyamine and the support. In comparison, Sayari et al.[17] reported a substantially lower uptake loss of 14% for TRI-PE-MCM-41-50/120 after 40 cycles, with the formation of urea species under CO_2 atmosphere and elevated temperatures as the main deterioration pathway. A later study showed that secondary amines are more stable than primary amines against CO_2-induced deactivation.[45] Urea formation from the amine groups can be greatly suppressed in the presence of steam[17] but requires a hydrothermally resistant support. It has been shown that commercialized Mg_xAl-CO_3 LDH-derived materials are highly stable during thousands of cycles for CO_2 adsorption in the presence of steam without structural collapse, even at elevated temperatures.[46] Our previous work also demonstrated that polyamine-functionalized calcined $Mg_{0.55}Al$-a lost 14% of the CO_2 capacity after 20 cycles under dry conditions, but were highly stable when regenerated by steam purging.[21] In addition, humid stream increases the CO_2 uptake by 36.7%, which is mainly ascribed to the shift of the adsorption mechanism to the formation of ammonium bicarbonate.

DISCUSSION

A novel class 2 adsorbent consisting of a monolayer of amine-tethered Mg-Al-CO_3 LDH-derived nanosheets was prepared and investigated for DAC by adsorption applications. In the first step, a series of LDH-derived nanosheets with tailored sizes and thicknesses were successfully synthesized. These LDH-derived nanosheets can be exfoliated into structures with considerably broader pore size distributions than ordered mesoporous silica. After functionalization under anhydrous conditions, amine monolayers were grafted onto the exposed hydroxyl groups of LDHs by silylation reactions. The platelet size and thickness of LDHs, as well as their morphologies, determine the amine loadings. For instance, bulk Mg_2Al-urea exhibited low amine loading, whereas $Mg_{0.55}Al$-a with ultrafine (20 nm) and ultrathin (2.50 nm) nanosheets and flower-like morphologies achieved an amine loading of 6.399 mmol g^{-1}. As a result, TRI-$Mg_{0.55}Al$-a showed a CO_2 adsorption capacity of 1.05 mmol g^{-1} at 25°C under 400 ppm CO_2, which is 30% higher than a TRI-modified SBA-15 support. APS-grafted $Mg_{0.55}Al$-a with only primary amines achieved the highest amine efficiency of 0.212.

Amine monolayer grafting also resulted in minimal changes to the support morphology and mitigated amine blockages, thus retaining high surface areas (162 m^2 g^{-1}) and pore volumes (0.553 cm^3 g^{-1}). Therefore, fast adsorption-desorption kinetics are obtained with these large CO_2 diffusion channels. Both the APS- and TRI-$Mg_{0.55}Al$-a reached 70% adsorption capacity within 30 min, and could be regenerated to 80% capacity in temperatures as low as 80°C. In addition, the strong chemical bond between the amines and LDHs, as well as the steam resistance, provide promising thermal, hydrothermal, and chemical stabilities. During a 50-cycle test with a short adsorption/desorption duration, TRI-$Mg_{0.55}Al$-a achieved a highly stable working capacity of 0.912 mmol g^{-1}. Considering the cheap and scalable production procedure, monolayer amine-grafted LDH-derived nanosheets should be highly attractive to build new R-TSA processes for DAC.

EXPERIMENTAL PROCEDURES

Resource availability

Lead contact

Further information and requests for resources and reagents should be directed to and will be fulfilled by the lead contact, Ruzhu Wang (rzwang@sjtu.edu.cn).

Materials availability

Modified LDHs generated in this study will be made available on request, but we may require a payment and/or a completed materials transfer agreement if there is potential for commercial application.

Data and code availability

Any additional information required to reanalyze the data reported in this article is available from the lead contact upon request.

Materials

All of the chemicals were used without further purification. $Mg(NO_3)_2 \cdot 6H_2O$ (analytical reagent [AR]), $Al(NO_3)_3 \cdot 9H_2O$ (AR), Na_2CO_3 (AR), NaOH (AR), urea (AR), acetone (AR), toluene (AR), hexane (AR), and methanol (AR) were purchased from Sinopharm Chemical Reagent. 3-Aminopropyltrimethoxysilane (APS, 97% pure) was purchased from Aladdin. TRI (95% pure) was purchased from Macklin. Branched PEI ($M_w \approx 600$, 99% pure) was purchased from Alfa Aesar. SBA-15 (NO: XFF01) was purchased from Nanjing XFNANO Materials Tech. Deionized (DI) water was used throughout the experiments.

Preparation of bulk LDHs

Bulk LDHs were synthesized using the hydrothermal urea method. The metal precursors (50 mmol) of $Mg(NO_3)_2 \cdot 6H_2O$ and $Al(NO_3)_3 \cdot 9H_2O$ and urea (100 mmol) were dissolved in 100 mL DI water. The mixture was placed in an autoclave and heated at 140°C for 12 h under magnetic stirring. The sediment was then filtered and thoroughly washed with DI water until the pH was close to 7, followed by vacuum drying at 60°C overnight. The prepared samples are denoted Mg_xAl-urea.

Preparation of stacked LDHs

Stacked Mg_xAl-CO_3 LDHs were synthesized using a coprecipitation method. Typically, 100 mL $Mg(NO_3)_2 \cdot 6H_2O$ and $Al(NO_3)_3 \cdot 9H_2O$ aqueous solution containing 1 M metal precursor was added over 60 min by syringe pump to aqueous Na_2CO_3 (0.5 M, 100 mL) with continuous stirring. The pH of the solution was adjusted to 10.0 ± 0.1 by dropping in NaOH solution (4 M). The mixture was left to stand at 25°C for 16 h, and subsequently filtered and thoroughly washed with DI water until the pH was close to 7. The wet LDH was then dried under vacuum overnight at 60°C. The prepared samples were denoted Mg_xAl-w.

Preparation of exfoliated LDHs

Exfoliated Mg_xAl-CO_3 LDHs (also referred to as AMO-LDHs) were synthesized using AMOST. In contrast to the conventional coprecipitation method, the wet LDH filter cake after water washing was treated with acetone (1,000 mL) and then suspended in acetone (600 mL) with magnetic stirring for 4 h at 25°C. The mixture was filtered and washed with acetone (400 mL) and then dried under vacuum at 60°C overnight. The prepared samples are denoted Mg_xAl-a.

Preparation of ultrafine LDHs

Ultrafine LDHs were synthesized using a fast coprecipitation method. An aqueous solution (40 mL) of $Mg(NO_3)_2 \cdot 6H_2O$ and $Al(NO_3)_3 \cdot 9H_2O$ containing 2.5 M metal precursor was rapidly poured (<10 s) into aqueous Na_2CO_3 (0.5 M, 100 mL). The pH of the solution was adjusted to 10.0 ± 0.1 by adding NaOH solution (4 M). The slurry was stirred for 30 min, filtered, and washed with or without AMOST treatment. The prepared samples are denoted Mg_xAl-w/a-F.

Preparation of amine-functionalized adsorbents

The amine monolayer was grafted onto the support by silylation under anhydrous conditions. In a glass tube, a support (0.2 g) was suspended in toluene (15 mL). Once dissolved, an aminosilane (0.6 mL, APS or TRI) was added dropwise and stirred for 15 min at 25°C. The glass tube was placed in an autoclave and heated at 85°C for 16 h with magnetic stirring. The sediment was separated by centrifugation, washed twice with toluene (20 mL), hexane (20 mL), and methanol (20 mL), and then dried under vacuum at 60°C overnight. The prepared samples are denoted APS/TRI support.

PEI was loaded onto the supports using a wet impregnation method. Typically, PEI (1 g) was dispersed in methanol (50 mL). After forming a homogeneous solution, a support (0.5 g) was submerged and stirred for 3 h at 25°C. The methanol was then removed by rotary evaporation under an N_2 blanket. The obtained solid was dried under vacuum overnight at 60°C. The prepared samples are denoted PEI support.

Materials characterization

The morphologies and element distributions were collected using SEM (MAIA3, TESCAN) equipped with an EDS detector and TEM (Talos L120C G2, Thermo Scientific). The surface functional groups were detected on a FTIR spectroscope (Nicolet iS5, Thermo Scientific) in transmission mode with a resolution of 4 cm^{-1} and 32 scans. The N_2 adsorption-desorption isotherms at 77 K were measured on a Micromeritics ASAP 2460 analyzer with an equilibration interval of 15 s. Surface area/pore size and pore volume were determined by the Brunauer-Emmett-Teller (BET) and the Barrett-Joyner-Halenda (BJH) desorption methods, and pore size distribution was analyzed by density functional theory (DFT) model. Pre-analysis, samples were degassed at 120°C under vacuum for 6 h. Quantitative analysis of N content was performed using a Vario EL Cube elemental analyzer.

CO_2 adsorption measurements

CO_2 adsorption isotherms were measured on a Micromeritics ASAP 2020 analyzer with an equilibration interval of 5 s. The operating temperature in the range of 25°C–65°C was controlled using an oil bath. Before analysis, the samples were degassed at 120°C under vacuum for 6 h.

CO_2 adsorption/desorption uptakes were tested on a PerkinElmer TGA 8000 thermogravimetric analyzer equipped with a 48-position autosampler and a water jacket, allowing fast heating and cooling (e.g., 50°C min^{-1}). In a typical test, ~5 mg of sample was loaded into a ceramic crucible and desorbed at 120°C under 90 mL min^{-1} of N_2 for 60 min. The temperature was then adjusted to an adsorption temperature of 25°C, followed by switching the inlet gas to 90 mL min^{-1} of 400 ppm CO_2 in N_2 for 120 min. The long-term stability was tested in a similar way with cyclic operation and shorter adsorption/desorption durations. In the TPD mode, the sample under 400 ppm CO_2 in N_2 was heated in pure N_2 from 25°C to 120°C at a heating rate of 5°C min^{-1}. The CO_2 concentration in the outlet gas was detected using a THA100S nondispersive infrared analyzer.

SUPPLEMENTAL INFORMATION

Supplemental information can be found online at https://doi.org/10.1016/j.xcrp.2021.100484.

ACKNOWLEDGMENTS

The research was supported by the National Natural Science Foundation of China (grant no. 52006135) and the Science and Technology Innovation Action Plan

Project of Shanghai (grant no. 20160712800). M.L. would like to acknowledge the China Scholarship Council (CSC) for a graduate scholarship. C.C. would like to thank SCG Chemicals of Thailand for financial support.

AUTHOR CONTRIBUTIONS

Conceptualization, X.Z. and M.L.; methodology, X.Z., M.L., and C.C.; investigation, X.Z. and J.W.; writing – original draft, X.Z. and M.L.; writing – review & editing, X.Z., C.C., F.Y., and D.O.; supervision, T.G., D.O., and R.W.; funding acquisition, X.Z. and T.G.

DECLARATION OF INTERESTS

The authors declare no competing interests.

Received: April 29, 2021
Revised: May 25, 2021
Accepted: June 8, 2021
Published: July 8, 2021

REFERENCES

1. Tiseo, L. (2021). Annual global emissions of carbon dioxide 2000–2019. https://www.statista.com/statistics/276629/global-co2-emissions/.
2. Koelbl, B.S., van den Broek, M.A., Faaij, A.P.C., and van Vuuren, D.P. (2014). Uncertainty in Carbon Capture and Storage (CCS) deployment projections: a cross-model comparison exercise. Clim. Change *123*, 461–476.
3. Rogelj, J., Luderer, G., Pietzcker, R.C., Kriegler, E., Schaeffer, M., Krey, V., and Riahi, K. (2015). Energy system transformations for limiting end-of-century warming to below 1.5 °C. Nat. Clim. Chang. *5*, 519–527.
4. Deutz, S., and Bardow, A. (2021). Life-cycle assessment of an industrial direct air capture process based on temperature–vacuum swing adsorption. Nat. Energy *6*, 203–213.
5. Keith, D.W., Holmes, G., St. Angelo, D., and Heidel, K. (2018). A process for capturing CO_2 from the atmosphere. Joule *2*, 1573–1594.
6. Sanz-Pérez, E.S., Murdock, C.R., Didas, S.A., and Jones, C.W. (2016). Direct capture of CO_2 from ambient air. Chem. Rev. *116*, 11840–11876.
7. Sutherland, B.R. (2019). Pricing CO_2 direct air capture. Joule *3*, 1571–1573.
8. Shi, X., Xiao, H., Kanamori, K., Yonezu, A., Lackner, K.S., and Chen, X. (2020). Moisture-driven CO_2 sorbents. Joule *4*, 1823–1837.
9. Jahandar Lashaki, M., Khiavi, S., and Sayari, A. (2019). Stability of amine-functionalized CO_2 adsorbents: a multifaceted puzzle. Chem. Soc. Rev. *48*, 3320–3405.
10. Shi, X., Xiao, H., Azarabadi, H., Song, J., Wu, X., Chen, X., and Lackner, K.S. (2020). Sorbents for the direct capture of CO_2 from ambient air. Angew. Chem. Int. Ed. Engl. *59*, 6984–7006.
11. Didas, S.A., Kulkarni, A.R., Sholl, D.S., and Jones, C.W. (2012). Role of amine structure on carbon dioxide adsorption from ultradilute gas streams such as ambient air. ChemSusChem *5*, 2058–2064.
12. Alkhabbaz, M.A., Bollini, P., Foo, G.S., Sievers, C., and Jones, C.W. (2014). Important roles of enthalpic and entropic contributions to CO_2 capture from simulated flue gas and ambient air using mesoporous silica grafted amines. J. Am. Chem. Soc. *136*, 13170–13173.
13. Brunelli, N.A., Didas, S.A., Venkatasubbaiah, K., and Jones, C.W. (2012). Tuning cooperativity by controlling the linker length of silica-supported amines in catalysis and CO_2 capture. J. Am. Chem. Soc. *134*, 13950–13953.
14. Harlick, P.J.E., and Sayari, A. (2006). Applications of pore-expanded mesoporous silicas. 3. Triamine silane grafting for enhanced CO_2 adsorption. Ind. Eng. Chem. Res. *45*, 3248–3255.
15. Harlick, P.J.E., and Sayari, A. (2007). Applications of pore-expanded mesoporous silica. 5. Triamine grafted material with exceptional CO_2 dynamic and equilibrium adsorption performance. Ind. Eng. Chem. Res. *46*, 446–458.
16. Belmabkhout, Y., Serna-Guerrero, R., and Sayari, A. (2010). Adsorption of CO_2-containing gas mixtures over amine-bearing pore-expanded MCM-41 silica: application for gas purification. Ind. Eng. Chem. Res. *49*, 359–365.
17. Sayari, A., and Belmabkhout, Y. (2010). Stabilization of amine-containing $CO_{(2)}$ adsorbents: dramatic effect of water vapor. J. Am. Chem. Soc. *132*, 6312–6314.
18. Yoo, C.J., Park, S.J., and Jones, C.W. (2020). CO_2 adsorption and oxidative degradation of silica-supported branched and linear aminosilanes. Ind. Eng. Chem. Res. *59*, 7061–7071.
19. Huang, H.Y., Yang, R.T., Chinn, D., and Munson, C.L. (2003). Amine-grafted MCM-48 and silica xerogel as superior sorbents for acidic gas removal from natural gas. Ind. Eng. Chem. Res. *42*, 2427–2433.
20. Stuckert, N.R., and Yang, R.T. (2011). CO_2 capture from the atmosphere and simultaneous concentration using zeolites and amine-grafted SBA-15. Environ. Sci. Technol. *45*, 10257–10264.
21. Zhu, X., Ge, T., Yang, F., Lyu, M., Chen, C., O'Hare, D., and Wang, R. (2020). Efficient CO_2 capture from ambient air with amine-functionalized Mg–Al mixed metal oxides. J. Mater. Chem. A Mater. Energy Sustain. *8*, 16421–16428.
22. Wang, Q., and O'Hare, D. (2013). Large-scale synthesis of highly dispersed layered double hydroxide powders containing delaminated single layer nanosheets. Chem. Commun. (Camb.) *49*, 6301–6303.
23. Chen, C., Yang, M., Wang, Q., Buffet, J.C., and O'Hare, D. (2014). Synthesis and characterisation of aqueous miscible organic-layered double hydroxides. J. Mater. Chem. A Mater. Energy Sustain. *2*, 15102–15110.
24. Chen, C., Wangriya, A., Buffet, J.C., and O'Hare, D. (2015). Tuneable ultra high specific surface area Mg/Al-CO_3 layered double hydroxides. Dalton Trans. *44*, 16392–16398.
25. Li, S., Ribeiro, A.M., Shi, Y., Moreira, M.N., Cai, N., and Rodrigues, A.E. (2015). Synthesis, pelleting, and performance evaluation of a novel K-promoted gamma-alumina/MgAl-layered double oxide composite adsorbent for warm gas H_2/CO_2 separation. Ind. Eng. Chem. Res. *54*, 7154–7163.
26. Li, S., Shi, Y., and Cai, N. (2015). Potassium-promoted gamma-alumina adsorbent from K_2CO_3 coagulated alumina sol for warm gas carbon dioxide separation. ACS Sustain. Chem. Eng. *3*, 111–116.
27. Zhao, Y., Zhao, Y., Waterhouse, G.I.N., Zheng, L., Cao, X., Teng, F., Wu, L.Z., Tung, C.H., O'Hare, D., and Zhang, T. (2017). Layered-double-hydroxide nanosheets as efficient

visible-light-driven photocatalysts for dinitrogen fixation. Adv. Mater. *29*, 1703828.

28. Park, A.Y., Kwon, H., Woo, A.J., and Kim, S.J. (2005). Layered double hydroxide surface modified with (3-aminopropyl)triethoxysilane by covalent bonding. Adv. Mater. *17*, 106–109.

29. Chen, C., Buffet, J.C., and O'Hare, D. (2020). Surface modification of aqueous miscible organic layered double hydroxides (AMO-LDHs). Dalton Trans. *49*, 8498–8503.

30. Zhu, X., Ge, T., Yang, F., and Wang, R. (2021). Design of steam-assisted temperature vacuum-swing adsorption processes for efficient CO_2 capture from ambient air. Renew. Sustain. Energy Rev. *137*, 110651.

31. Azarabadi, H., and Lackner, K.S. (2019). A sorbent-focused techno-economic analysis of direct air capture. Appl. Energy *250*, 959–975.

32. Bali, S., Leisen, J., Foo, G.S., Sievers, C., and Jones, C.W. (2014). Aminosilanes grafted to basic alumina as CO_2 adsorbents–role of grafting conditions on CO_2 adsorption properties. ChemSusChem *7*, 3145–3156.

33. Didas, S.A., Sakwa-Novak, M.A., Foo, G.S., Sievers, C., and Jones, C.W. (2014). Effect of amine surface coverage on the co-adsorption of CO_2 and water: spectral deconvolution of adsorbed species. J. Phys. Chem. Lett. *5*, 4194–4200.

34. Zhang, Q., Guo, Y., Leroux, F., Tang, P., Li, D., Wang, L., and Feng, Y. (2020). An aqueous miscible organic (AMO) process for layered double hydroxides (LDHs) for the enhanced properties of polypropylene/LDH composites. New J. Chem. *44*, 10119–10126.

35. Potter, M.E., Cho, K.M., Lee, J.J., and Jones, C.W. (2017). Role of alumina basicity in CO_2 uptake in 3-aminopropylsilyl-grafted alumina adsorbents. ChemSusChem *10*, 2192–2201.

36. McDonald, T.M., Lee, W.R., Mason, J.A., Wiers, B.M., Hong, C.S., and Long, J.R. (2012). Capture of carbon dioxide from air and flue gas in the alkylamine-appended metal-organic framework mmen-Mg_2(dobpdc). J. Am. Chem. Soc. *134*, 7056–7065.

37. Choi, S., Gray, M.L., and Jones, C.W. (2011). Amine-tethered solid adsorbents coupling high adsorption capacity and regenerability for CO_2 capture from ambient air. ChemSusChem *4*, 628–635.

38. Holewinski, A., Sakwa-Novak, M.A., and Jones, C.W. (2015). Linking CO_2 sorption performance to polymer morphology in aminopolymer/silica composites through neutron scattering. J. Am. Chem. Soc. *137*, 11749–11759.

39. Sayari, A., Heydari-Gorji, A., and Yang, Y. (2012). CO_2-induced degradation of amine-containing adsorbents: reaction products and pathways. J. Am. Chem. Soc. *134*, 13834–13842.

40. Wilfong, W.C., Kail, B.W., Jones, C.W., Pacheco, C., and Gray, M.L. (2016). Spectroscopic investigation of the mechanisms responsible for the superior stability of hybrid class 1/class 2 CO_2 sorbents: a new class 4 category. ACS Appl. Mater. Interfaces *8*, 12780–12791.

41. Sakwa-Novak, M.A., Tan, S., and Jones, C.W. (2015). Role of additives in composite PEI/oxide CO_2 adsorbents: enhancement in the amine efficiency of supported PEI by PEG in CO_2 capture from simulated ambient air. ACS Appl. Mater. Interfaces *7*, 24748–24759.

42. Kuwahara, Y., Kang, D.Y., Copeland, J.R., Brunelli, N.A., Didas, S.A., Bollini, P., Sievers, C., Kamegawa, T., Yamashita, H., and Jones, C.W. (2012). Dramatic enhancement of CO_2 uptake by poly(ethyleneimine) using zirconosilicate supports. J. Am. Chem. Soc. *134*, 10757–10760.

43. Kuwahara, Y., Kang, D.Y., Copeland, J.R., Bollini, P., Sievers, C., Kamegawa, T., Yamashita, H., and Jones, C.W. (2012). Enhanced CO_2 adsorption over polymeric amines supported on heteroatom-incorporated SBA-15 silica: impact of heteroatom type and loading on sorbent structure and adsorption performance. Chemistry *18*, 16649–16664.

44. Sayari, A., Liu, Q., and Mishra, P. (2016). Enhanced adsorption efficiency through materials design for direct air capture over supported polyethylenimine. ChemSusChem *9*, 2796–2803.

45. Sayari, A., Belmabkhout, Y., and Da'na, E. (2012). CO_2 deactivation of supported amines: does the nature of amine matter? Langmuir *28*, 4241–4247.

46. Zhu, X., Li, S., Shi, Y., and Cai, N. (2019). Recent advances in elevated-temperature pressure swing adsorption for carbon capture and hydrogen production. Prog. Energ. Combust. *75*, 100784.